ACS OMEGA

Open Access

http://pubs.acs.org/journal/acsodf

Review

Role of Electrical Conductivity in the Shielding Effectiveness of Composite Polyvinyl Alcohol/Multiwall Carbon Nanotube Nanofibers for Electromagnetic Interference Applications

Waleed Ghafoor, Mashhood Ahmad,* Muhammad Raffi, and Saif Ullah Awan

Cite This: *ACS Omega* 2024, 9, 3070−3077

Read Online

ACCESS | Metrics & More | Article Recommendations

ABSTRACT: The shielding effectiveness (SE) against the electromagnetic interference (EMI) of polyvinyl alcohol/multiwall carbon nanotubes (PVA/MWCNTs) composite nanofibers is characteristic of higher absorptivity of the radiation that enhances with the increasing concentration of MWCNTs content in these composites. However, by enriching the content of conductive fillers (MWCNTs), the conductivity of the composites is also stirred up. Concomitantly, the conductivity of these composites contributes toward the reflectivity of the EM radiation from them. Certain applications of the EMI shielding material require a lower level of reflectivity of the EM radiation. This study intends to see how SE of the PVA/MWCNTs composite nanofibers is affected vis-a-vis their conductivity for S-band radiation. Samples of nanofibers, with (5, 10, 15, and 20) wt % of MWCNTs loading in 10 wt % of PVA solution, were prepared through electrospinning and studied for their electrical conductivity and EMI SE. It is observed that by increasing the content of MWCNTs in PVA solution from 5 to 20 wt % the conductivity of the composites tends to increase from 21 to 866 times that of PVA, while the SE increases from 10 db to 25 db over the S-band range of frequencies.

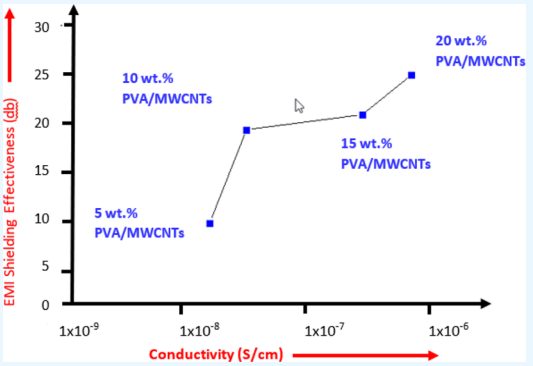

1. INTRODUCTION

The advancements in the miniaturization of electrical and electronic devices have introduced a type of electronic pollution termed as electromagnetic interference (EMI).[1] This interference hinders the working of the electronic devices and perturbs their operation. There is a need to develop a mechanism for shielding these devices from EMI. Conducting materials like metals are considered good shielding materials against EMI.[2] The most commonly used metals for this purpose are aluminum, silver, copper, and tantalum. The conductivity of these metals is owed much to the presence of excess free electrons in them. However, metals have their own limitations such as corrosion, low flexibility, and heavy weight. The lightweight materials like plastics are also considered to be a good choice for EMI shielding.[2] By introducing small traces of the conductive filler, during the process of preparation of these materials, a certain conductivity may be introduced in these plastic composites. Therefore, a composite of a polymer and a conductive filler may be used as a shielding material to reduce the EMI.[2−5] Normally a long polymer chain matrix is mixed with a conductive filler to make a composite of desired properties.[6] A composite of polymer is also useful in enhancing the physical, electrical, and mechanical properties of the materials. The ease of processability, low weight, high flexibility, and high corrosion resistance are a few advantages of these plastic composites over metals. Polymers and carbon nanotubes-based composites have the advantage of blocking electromagnetic radiation and are being widely studied for their use in EMI control applications.

Polyvinyl alcohol (PVA) is a low-cost, odorless, and nontoxic polymer having excellent film-forming, emulsifying and adhesive properties. It is a dielectric, thermostable, transparent, semicrystalline, biodegradable, water-soluble, biocompatible, and environmentally friendly polymer having good physical properties and chemical stability. PVA films and adhesives have excellent chemical and physical resistances. On the other hand, multiwall carbon nanotubes (MWCNTs) have a direct bandgap of 2.7−3 eV. These have high thermal stability, high breakdown field, environment friendly characteristics, moderately low cost, and excellent thermal and electrical conductivities. As a result, PVA/MWCNTs composites are low-cost and lightweight nanofibers having good processability, good tensile strength, high thermal stability, low chemical

Received: June 10, 2023
Revised: October 8, 2023
Accepted: October 11, 2023
Published: January 5, 2024

toxicity, high specific surface area, and tunable conductivities over a wide range of frequencies. Thus, PVA/MWCNTs are advantageous materials for high-performance EMI shielding applications.

Electrospinning is the most widely used technique for the synthesis of nanofibers from polymeric solutions. However, due to their large aspect ratio, MWCNTs are prone to agglomerate in the polymeric solution, so a complex dispersion process is required in preparation of PVA/MWCNTs nanofibers with a smooth surface. Depending upon the relevant strengths of the viscoelastic and electrostatic forces in the composite solution, the diameter and smoothness of the resulting nanofibers increases or decreases with the MWCNTs' content in the solution.[7−15] A focused investigation into the process of synthesis of PVA/MWCNTs composite nanofibers is reported in the literature.[16−23]

The EMI shielding characteristic of PVA/MWCNTs composites is mainly due to absorption and reflection mechanisms. With the enhancement of MWCNTs filler content in the base polymer material, both the radiation absorptivity and conductivity of the composite nanofibers tend to increase. Besides the frequency of the EM waves and other parameters of the polymer composite materials, the structural defects are considered major contributors toward their radiation absorptivity, while their radiation reflectivity is associated with their conductivity. Thus, by enhancing the MWCNTs' filler content, both the structural defects and conductivity of PVA/MWCNTs nanofibers upsurge, augmenting their shielding effectiveness (SE).[24,25] By employing response surface methodology (RSM), empirical models of the carbon nanotubes/polymer composite nanofibers have been proposed. These models put forward some correlations between the SE of these composites and certain material parameters like conductivity and thickness of the samples.[26,27]

In this study, electrospun nanofibers of PVA/MWCNTs with different concentrations (5, 10, 15, and 20) wt % of MWCNTs are discussed as EMI shielding materials for a (S-band) range of frequencies of EM waves. The optimum values of SE of different samples of PVA/MWCNTs were observed at a 4 GHz frequency. The variation in the optimum value of SE of these samples is compared with the change in electrical conductivity of the samples vas-a-vis MWCNTs content in the samples. This comparison reveals that the rise in conductivity value results in the rise in SE of PVA/MWCNTs composites with the increasing content of MWCNTs in the PVA/MWCNTs composites.

2. EXPERIMENTAL SECTION

2.1. Preparation of PVA/MWCNTs Composite Nanofibers. The 10 wt % polyvinyl alcohol of molecular weight (MW) 89000−98000 g/mol with a degree of hydrolysis of 99+% (product code: 1001891395 and obtained from Sigma-Aldrich) was dissolved in deionized water. Multiwalled carbon nanotubes of purity >90% (obtained from Carbon Nanomaterial Technology, South Korea) were used. All the equipment used in making the composite solution was washed and cleaned ultrasonically using deionized water. Sodium dodecyl sulfate (SDS) of MW 288.38 g/mol and 92.5−100.5% based on total alkyl sulfate content (lot BCBL8758 V from Sigma-Aldrich) were used as a surfactant for the dispersion of MWCNTs in the solution. 1 wt % sodium dodecyl sulfate (SDS) was dissolved in 3 mL of deionized water solution. The solution was continuously stirred and heated for 1 h at around 25 °C. After this, a known weight percent of MWCNTs acquired from Carbon Nanomaterial Technology, South Korea was added in the 3 mL solution. Owing to the van der Waals interaction between the atoms of MWCNTs, these appear in the form of bundles, making it difficult to disperse these in the aqueous solution. A very small amount of surfactant SDS was added in the solution before MWCNTs were added. For the dispersion of MWCNTs in aqueous solution, a surfactant and a high shear force ultrasonic liquid processor were used. The solution was ultrasonicated by an ultrasonic liquid processor (ULP-750) for 20 min. An ultrasonic device was used to disperse the carbon nanotubes using high impact energy and to dissolve the MWCNTs in aqueous solution. The MWCNTs interacted with the hydrophobic tail of sodium dodecyl sulfate, while the hydrophilic headgroup got associated with the water. Both the ultrasonication and sodium dodecyl sulfate were used to reduce the van der Waals interaction between the atoms of MWCNTs. After the ultrasonication of the solution, 10 wt % polyvinyl alcohol (PVA) was added to the solution. The solution was heated for 2 h at 80 °C. The MWCNTs solution and PVA were mixed by using a magnetic stirrer and heating system. The beaker containing the solution was covered with aluminum foil in order to prevent the solution from vaporizing at high temperature. A viscous solution of the poly(vinyl alcohol)/sodium dodecyl sulfate/multiwall carbon nanotubes was obtained after 2 h of continuous stirring and heating. Nanocomposite nanofibers with different loadings of MWCNTs (i.e., 5, 10,15 and 20%) were prepared to study their effect on crystallinity, morphology, electrical conductivity, and shielding effectiveness. The amounts of materials used for making the composite solution and the number of the samples prepared are described as under in Table 1.

Table 1. Amounts of Materials Used for Making Composite Solution

sample	deionized H_2O (g)	PVA (g)	SDS (g)	MWCNTs (g)
1	3	0.3	0	0
2	3	0.3	0.03	0.015
3	3	0.3	0.03	0.03
4	3	0.3	0.03	0.045
5	3	0.3	0.03	0.06

The composite solution was prepared and fed into the syringe pump. The DC voltage up to 50 kV was generated by a high power supply. One electrode of high DC potential was attached to the nozzle of the syringe, while the other grounded electrode was connected to the collector. For the synthesis of nanofibers from electrospinning, the DC potential was set up to 19 kV, and the distance between the needle of the syringe and collector was chosen equal to 11 cm. For the stable electrospinning process, the liquid flow rate was set around 1 mL/h. The PVA/MWCNTs composite nanofibers were prepared under the optimized conditions. A rotating drum was used as a collector for the collection of nanofibers. The speed of this rotating drum was controlled by using a pulse width modulated circuit that controlled the speed of the motor. The rpm of the rotating drum ranged between 1500 and 2000.

2.2. Characterization Techniques. The moisture free samples of PVA/MWCNTs nanofibers were used for different types of characterizations. The samples were peeled off, cut into small straps, and coated with the gold before the SEM

https://doi.org/10.1021/acsomega.3c04120
ACS Omega 2024, 9, 3070−3077

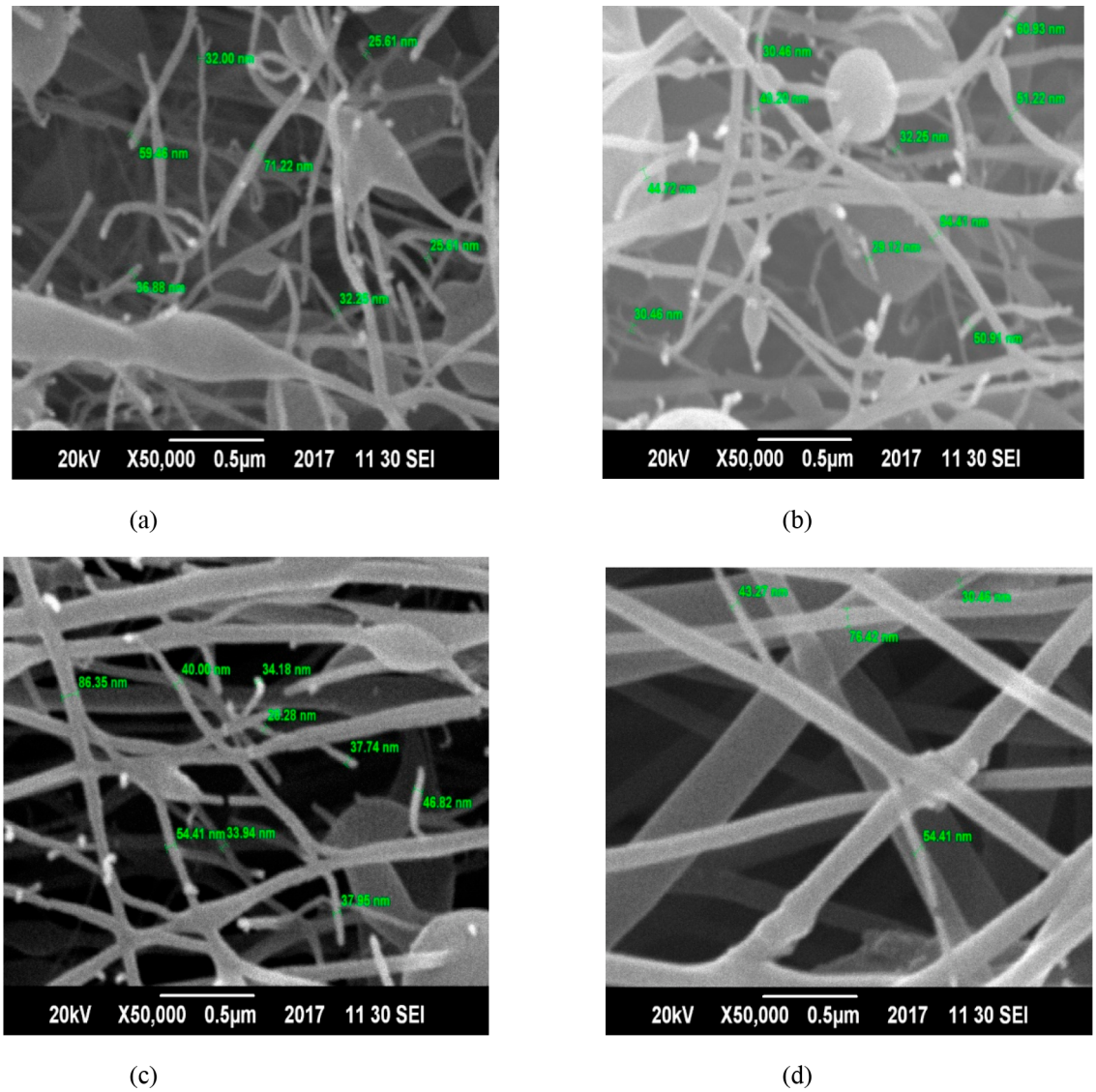

Figure 1. SEM micrographs of PVA/MWCNTs composite nanofibers (a) pure PVA, (b) 5 wt %, (c) 10 wt %, (d) 20 wt % MWCNTs loading in PVA prepared with 3 mL of solvent at ×50,000 magnification.

analysis of their surface morphology. The diameter of the nanofibers was estimated from the SEM micrographs. The crystal structure of PVA/MWCNTs composite nanofibers was revealed from the XRD analysis. The crystallite size and dislocation density were also estimated from this analysis. Fourier transform infrared (FTIR) spectroscopy of the PVA/MWCNTs composite nanofibers revealed the bonding behaviors among their atoms. The conductivity of the PVA/MWCNTs composite nanofibers was carried out by using the Four Point Probe Van der Pauw method. For the thickness measurement of all the samples, a 2D noncontact optical profilometer was used. Consequently, the conductivity of the samples got measured. Finally, the EMI SE of the prepared samples was carried out by measuring their scattering parameters with a vector network analyzer for the S-band range of frequencies.

3. RESULTS AND DISCUSSION

3.1. SEM Analysis. The SEM micrographs reflect the successful synthesis of the PVA/MWCNTs composite nanofibers. Figure 1a gives the SEM micrograph of pure PVA nanofibers, while Figure 1b–d reflects the micrographs of PVA/MWCNTs composite nanofibers with (5, 10, and 20 wt %) loading of MWCNTs in PVA. All of these micrographs are shown at magnification ×50,000. Figure 1a electrospun PVA nanofibers appear with portions of beading. The quality of these nanofibers is seen to be low in comparison to that of PVA/MWCNTs composite nanofibers. The diameter of pure PVA nanofibers is found to be within the range of 25–75 nm. In Figure 1b, the nanofibers of sample with 5 wt % of MWCNTs in PVA result in small portions of beading. It is due to the low dispersion of MWCNTs in PVA solution. The agglomerating forms of nanofibers are owed to improper mixing of MWCNTs in PVA solution. The diameter of these nanofibers is found to be within the range of 20–70 nm. Figure 1c gives the nanofibers of PVA/MWCNTs composite with 10 wt % of MWCNTs in PVA. The quality of the nanofibers is quite improved in this case in comparison to that of those discussed in two previous cases Figure 1a,b. The diameter of the nanofibers in this case is found in range between 25 and 90 nm. Nanofibers with excellent quality, without any beadings, are shown in the SEM micrograph of Figure 1d. The

https://doi.org/10.1021/acsomega.3c04120
ACS Omega 2024, 9, 3070−3077

nanofibers in this case are of PVA/MWCNTs composite with 20 wt % loading of MWCNTs in PVA. Due to the increased content of MWCNTs, the viscosity of the composite solution was increased. As the 20 wt % composite solution is more viscous compared with 5 and 10 wt % solutions, the electrospinning of this solution produced more stable jet flow during the synthesis of nanofibers resulting in the production of smoother and beadless nanofibers. The diameter of these composite nanofibers is found in the range between 30 and 80 nm. It is observed that by increasing wt % of MWCNTs in PVA/MWCNTs composites, smoother and beadless nanofibers got formed. With the increasing content of MWCNTs not only the refinement of the fibers improves but also the SE as well as the conductivity of the samples gets improved.

3.2. FTIR Spectroscopy. The purity of contents of PVA solution with MWCNTs was confirmed by structural analysis of electrospun PVA/MWCNTs composite nanofibers. This analysis was carried out by using Fourier Transform Infrared (FTIR) spectroscopy. The FTIR spectra of the pure PVA nanofibers and the PVA/MWCNTs composite nanofibers with loading of 5, 10, 15, and 20 wt % are shown in Figure 2. In

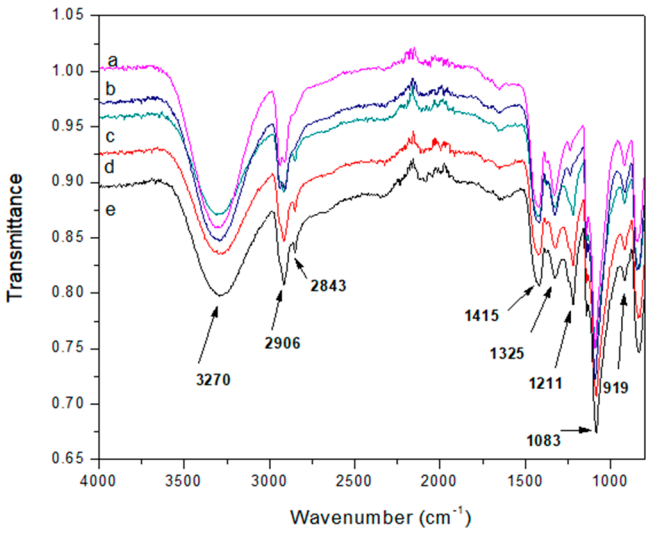

Figure 2. FTIR spectra of (a) pure PVA nanofibers, (b) 5 wt % PVA/MWCNTs, (c) 10 wt % PVA/MWCNTs, (d) 15 wt % PVA/MWCNTs, (e) 20 wt % PVA/MWCNTs.

Figure 2 all of the plots (a–e) give the main characteristic transmittance peak around 3270 cm^{-1}, which depicts the presence of an alcoholic functional group in the material. The band at 3270 cm^{-1} is the O–H stretching mode, while peaks at 2906 cm^{-1} correspond to the C–H stretching. In Figure 2, the peak at around 2843 cm^{-1} is attributed to the CH_2 bond stretching. The C–H bond stretching is observed at 1415 cm^{-1}. Other peaks, at 1325 cm^{-1} are associated with CH–OH bending, at 1211 cm^{-1} with C–H wagging and at 1083 cm^{-1} with C–O stretching. It is observed that the positions of these peaks are almost same in all samples with only difference in their intensities. Polyvinyl alcohol nanofibers samples contain an OH functional group. The PVA is present in all samples, so the OH transmittance peak is observed in all samples. So, for pure PVA nanofibers, this peak has maximum transmittance as compared to samples loaded with MWCNTs. The intensity of this OH peak tends to decrease in samples of 5, 10, 15 and 20 wt % because of increasing content of MWCNTs in PVA.

3.3. XRD Analysis. The XRD analysis of the samples measured the effect on the crystallinity of PVA/MWCNTs by varying the content of MWCNTs in the PVA nanofibers. The crystallite size and dislocation density of the composite nanofibers were calculated from this analysis. Figure 3 shows

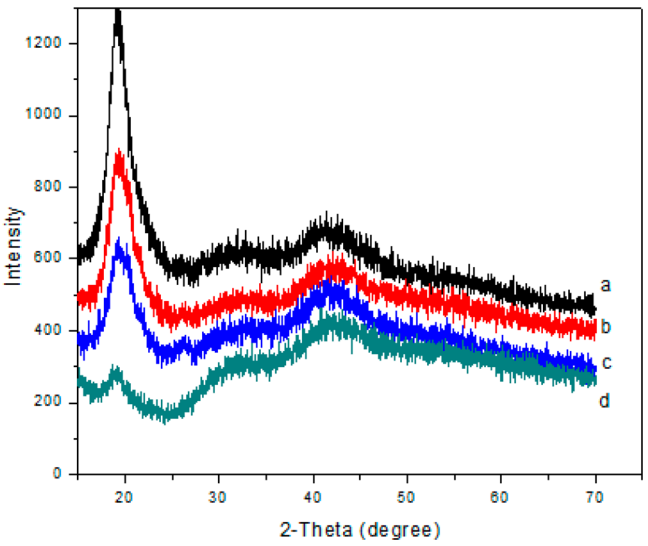

Figure 3. XRD spectra of (a) 5 wt % MWCNTs in PVA, (b) 10 wt % MWCNTs in PVA, (c) 20 wt % MWCNTs in PVA, (d) pure PVA nanofibers.

the X-ray diffraction pattern of pure PVA nanofibers and PVA/MWCNTs composite nanofibers under different loadings of MWCNTs (i.e., 5, 10, 20 wt %). The XRD spectra are plotted for 2θ range from 15 to 75°. For pure PVA nanofibers, the main characteristic peak is observed at around 2θ = 19.238°. This peak corresponds to presence of a (110) plane of atoms in PVA.[28−30] For samples containing 5, 10, and 20 wt % MWCNT in PVA, an increase in the broadness and decrease in the intensity of the peaks are observed. This corresponds to the amorphous behavior of a new kind of PVA/MWCNTs composite material. The decrease in the crystallinity is observed by adding more content of MWCNTs. The main characteristic peak for all the samples observed at different diffraction angles is specified in Table 2. The crystallite size and dislocation density values are also shown in this table. The crystallite size is calculated by using Scherrer's relation. The

Table 2. Crystallite Size and Dislocation Density Calculations of Samples

sample	diffraction angle 2θ	fwhm	crystallite size D (nm)	Dislocation density (nm^{-2})
5 wt % PVA/MWCNT nanofibers	19.309°	1.006	8.37	1.427×10^{-2}
10 wt % PVA/MWCNTs nanofibers	19.532°	0.755	11.16	8.029×10^{-3}
20 wt % PVA/MWCNTs nanofibers	19.634°	0.721	13.25	5.69×10^{-3}
pure PVA nanofibers	19.151°	0.556	15.14	5.69×10^{-3}

https://doi.org/10.1021/acsomega.3c04120
ACS Omega 2024, 9, 3070−3077

crystallite size tends to increase due to the addition of more content of MWCNTs in PVA.

3.4. Electrical Conductivity and Shielding Effectiveness. After the samples were dried for 24 h, four metal contacts of silver were pasted on the corners of each sample. Thickness of each sample was measured by a 2D non-contact optical profilometer, as a function of different concentrations of MWCNTs. The resistivity (ρ) of the samples bears a direct relationship with the thickness (t) of the samples and is given as

$$\rho = \frac{\pi}{\ln(2)} t \left(\frac{V}{I}\right) \quad (1)$$

The inverse values of the resistivity give the conductivity values of the samples. The conductivity of the pure PVA was found to be on the order of 7.75×10^{-10} S/cm. This value of conductivity reflects that the PVA nanofibers are showing insulator behavior. The conductivity of the composites tends to increase by adding more contents of MWCNTs to the maximum order of 866 times that of PVA. The details of the results of the four probe van der Pauw measurements are reflected in Table 3. The highest conductivity on the order of 6.71×10^{-7} is achieved for the sample with 20 wt % MWCNTs immersed in PVA. It is predicted that the conductivity may be further enhanced by submerging more contents of MWCNTs in PVA. These results are depicted graphically in Figure 4.

Table 3. Values of Conductivity under Different Loadings of MWCNTs

sample	thickness (cm)	resistivity ρ (Ω-cm)	conductivity σ (S/cm)
PVA	7.553×10^{-4}	1.29×10^{9}	7.75×10^{-10}
5 wt % MWCNT	2.5391×10^{-3}	6.2×10^{7}	1.61×10^{-8}
10 wt % MWCNT	2.391×10^{-3}	3.14×10^{7}	3.18×10^{-8}
15 wt % MWCNTs	6.573×10^{-3}	3.68×10^{6}	2.717×10^{-7}
20 wt % MWCNT	4.1789×10^{-3}	1.49×10^{6}	6.71×10^{-7}

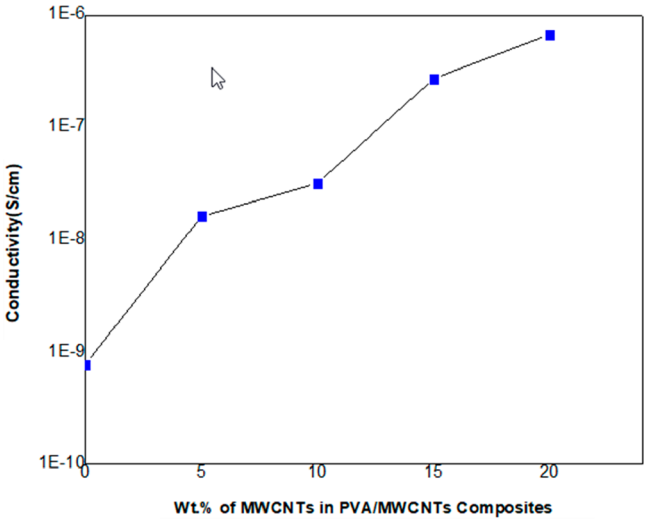

Figure 4. Effect on electrical conductivity of PVA/MWCNTs composite nanofibers under different loadings of MWCNTs using the Four-point probe method.

The ratio of the incident to transmitted electric field strengths expressed in decibels quantifies the shielding effectiveness of the materials. If E_i is the intensity of the incident electromagnetic field and E_t is the intensity of the transmitted field, then the shielding effectiveness of the PVA/MWCNTs composite nanofibers is defined as[31]

$$SE = 20 \log|E_i/E_t| \quad (2)$$

The total shielding effect of the material samples is the sum total of shielding effectiveness due to radiation reflection, absorption, and multiple reflections inside the material surfaces. The collective impact of these effects gives overall shielding effectiveness quantified as

$$SE = SE_R + SE_A + SE_M \quad (3)$$

In terms of the reflection and transmission coefficients (i.e., scattering parameters), the shielding effectiveness of the samples is given as

$$SE = 20 \log \sqrt{\frac{1}{1 - |S_{12}|^2}} + 20 \log \sqrt{\frac{1 - |S_{11}|^2}{|S_{12}|^2}} + 20 \log[1 - \Gamma_1^2 e^{-2\gamma t}] \quad (4)$$

where $\Gamma_1 = \chi \pm \sqrt{\chi^2 - 1}$, $\chi = (S_{11}^2 - S_{21}^2 + 1)/2S_{11}^2$, and $e^{-\gamma t} = (S_{11} + S_{21} - \Gamma_1)/(1 - (S_{11} + S_{21})\Gamma_1)$.

The reflection coefficient S_{11} (or S_{22}) and transmission coefficient S_{21} (or S_{12}) are defined as

$$S_{11} = E_r/E_i \quad (5)$$

$$S_{21} = E_t/E_i \quad (6)$$

where E_r is the reflected electric field. By using a vector network analyzer, the scattering parameters of the electromagnetic radiation in 1−20 GHz range are plotted as a function of frequency in Figure 5, showing the plots of these transmission and reflection parameters for different loading of MWCNTs in PVA. Figure 5a reflects that for the sample containing 5 wt % MWCNTs load in PVA the maximum shielding effectiveness of 10 db is achieved for the frequency value around 4 GHz. By increasing the MWCNTs content to 10 wt % in PVA, the corresponding plot of Figure 5b reflects that the shielding effectiveness of 19 db is achieved at 4 GHz. Figure 5c reflects that the EMI shielding effectiveness of 21 db is achieved for the 15 wt % MWCNTs loading in PVA at the same frequency. The maximum shielding effectiveness of 25 db is achieved for the sample containing 20 wt % MWCNTs loading in PVA, at a frequency of 4 GHz. Thus, at a 4 GHz frequency, the samples of PVA with different loadings of MWCNTs show the optimum shielding effectiveness. The shielding effectiveness of PVA/MWCNTs composites got enhanced with the increasing conductivity of the samples.

By making use of response surface methodology (RSM), the reflective and absorptive parts of the SE are associated with the conductivity of the PVA/MWCNTs composites as under:

$$SE_R = 39.5 + 10 \log(\sigma/2\pi f\mu) \quad (7)$$

$$SE_A = 8.7t(\pi f\mu\sigma)^{1/2} \quad (8)$$

where t is the thickness of the PVA/MWCNTs samples, f is the frequency of the electromagnetic radiation, μ is the permeability of the composite material, and σ is the electrical conductivity of the samples. Along with eqs 7 and 8, eq 3

https://doi.org/10.1021/acsomega.3c04120
ACS Omega 2024, 9, 3070−3077

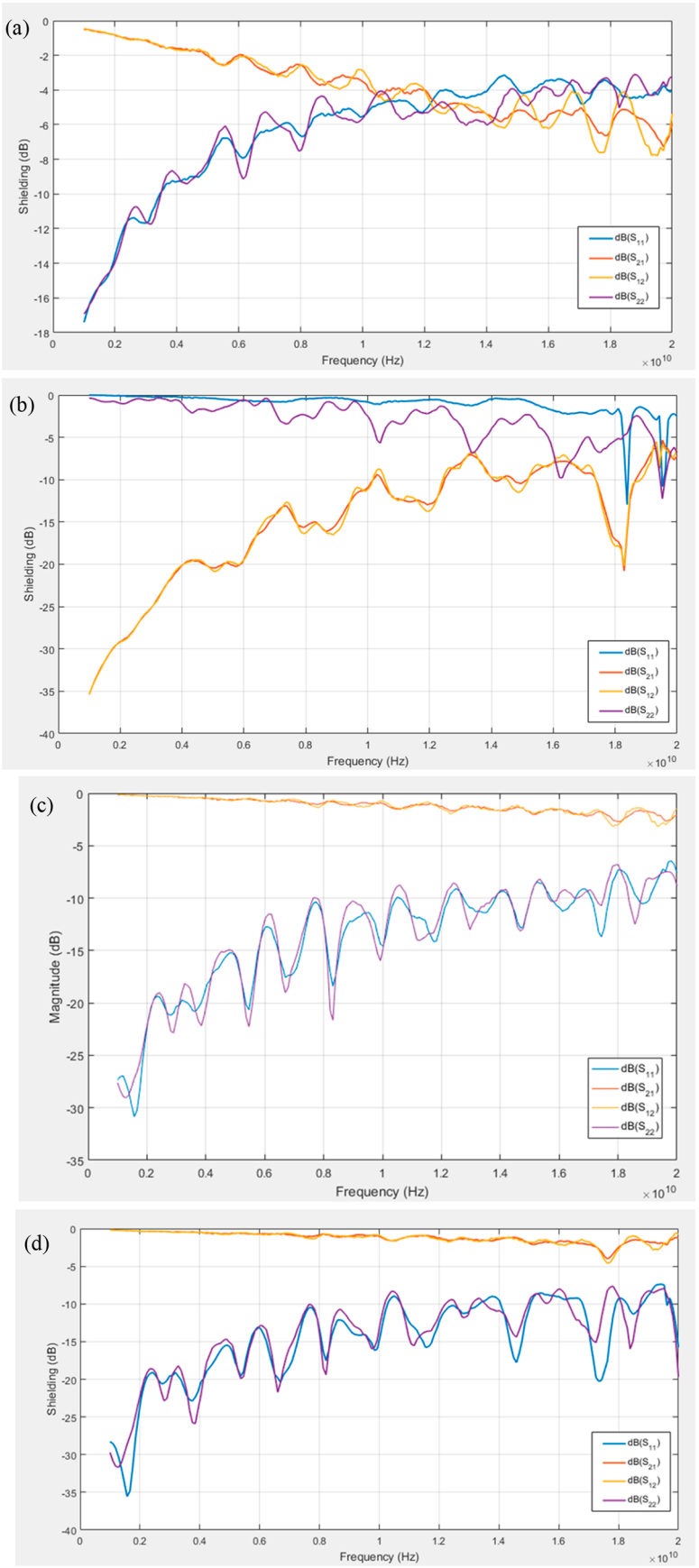

Figure 5. Shielding effectiveness of PVA/MWCNTs composite nanofibers under loading of (a) 5 wt %, (b) 10 wt %, (c) 15 wt %, (d) 20 wt %.

https://doi.org/10.1021/acsomega.3c04120
ACS Omega 2024, 9, 3070−3077

depicts a uniform relationship of shielding SE with the conductivity of the PVA/MWCNTs composites. However, the experimentally measured results of SE and the conductivity of the PVA/PWCNTs samples with different loading concentrations of MWCNTs in PVA are reflected in Table 4 and are

Table 4. Values of Shielding Effectiveness and Conductivity Per Unit Length for Different Samples

sample	thickness t (cm)	conductivity σ (S/cm)	shielding effectiveness (db)
5 wt % MWCNTs	2.539×10^{-3}	1.61×10^{-8}	10
10 wt % MWCNTs	2.391×10^{-3}	3.18×10^{-8}	19
15 wt % MWCNTs	6.573×10^{-3}	2.72×10^{-7}	21
20 wt % MWCNTs	4.179×10^{-3}	6.71×10^{-7}	25

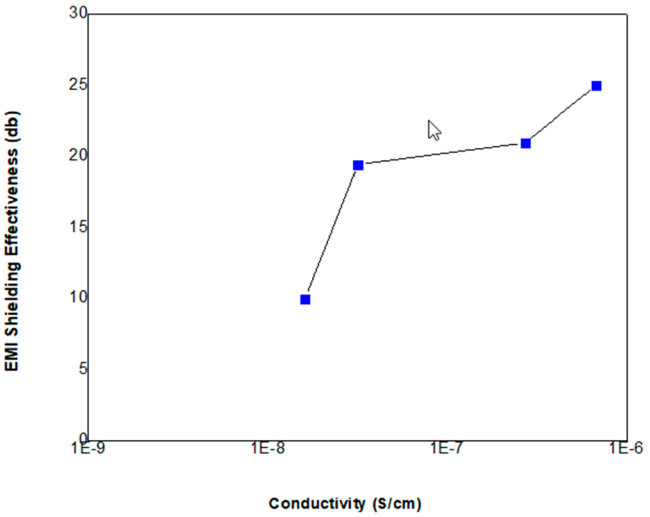

Figure 6. Optimum shielding effectiveness versus conductivity of PVA/MWCNTs composite nanofibers noted at loading percentages of MWCNTs in PVA, i.e., at 5 wt %, 10, 15, and 20 wt %.

plotted in Figure 6. The measurements of thickness of the samples are carried out through a 2D noncontact optical profilometer. It is observed that with the increment of MWCNTs content in the PVA/MWCNTs composite nanofibers the conductivity of the PVA/MWCNTs nanofibers is enhanced following the almost similar pattern as that of SE. This congruency in conductivity and SE of the PVA/MWCNTs composite nanofibers is expected even further for higher concentrations of MWCNTs content in the composite PVA/MWCNTs nanofibers and for a range of frequencies higher from the S-band.

4. CONCLUSION

In this study the morphology, structure analysis, electrical conductivity, and SE of PVA/MWCNTs composite nanofibers under different loadings of MWCNTs in PVA/MWCNTs composites were investigated to see the reliance of SE upon the conductivity of these samples. It is observed from the characterization results that those nanofibers of excellent quality are synthesized for the higher loading percentage of MWCNTs in PVA.

FTIR spectrum analysis of the composite nanofibers established the purity of the contents of the composites of the PVA with the MWCNTs. The decrease in the crystallinity in the samples was also observed due to more contents of MWCNTs in PVA. The electrical conductivity of PVA/MWCNTs composite nanofibers tends to increase from 21 to 866 times from that of PVA by increasing the content of MWCNTs from 5 wt % to 20 wt % in PVA/MWCNTs composites. Similarly, for this rise of concentration of MWCNTs content (5 wt % to 20 wt %), the optimum value of SE of the samples is found to increase from 10 to 25 db at 4 GHz frequency. Therefore, a rise in conductivity of the nanofibers results in a rise of SE of PVA/MWCNTs composites over the S-band range of frequencies. This trend appears to be followed even for higher concentrations of MWCNTs content in PVA and at frequencies higher than the S-band.

AUTHOR INFORMATION

Corresponding Author

Mashhood Ahmad − *Department of Electrical Engineering, NUST College of Electrical and Mechanical Engineering, National University of Sciences and Technology (NUST), Islamabad 4400, Pakistan;* orcid.org/0009-0007-9105-0079; Email: mashhood_ahmad@ceme.nust.edu.pk

Authors

Waleed Ghafoor − *Department of Electrical Engineering, NUST College of Electrical and Mechanical Engineering, National University of Sciences and Technology (NUST), Islamabad 4400, Pakistan*

Muhammad Raffi − *Department of Material Sciences, National Institute of Lasers and Optronics (NILOP), Islamabad 45650, Pakistan*

Saif Ullah Awan − *Department of Electrical Engineering, NUST College of Electrical and Mechanical Engineering, National University of Sciences and Technology (NUST), Islamabad 4400, Pakistan;* orcid.org/0000-0003-3370-3880

Complete contact information is available at: https://pubs.acs.org/10.1021/acsomega.3c04120

Notes

The authors declare no competing financial interest.

ACKNOWLEDGMENTS

The authors acknowledge the Materials Lab, NUST School of Natural Sciences (SNS) for extending their facility for carrying out FTIR spectroscopy of the samples, Advanced Energy Materials and Systems (AEMS) Lab, NUST US-Pakistan Center for Advanced Studies in Energy for extending their facility for carrying out XRD and SEM analyses of the samples and the Electromagnetic Compatibility/Electromagnetic Interference (EMC/EMI) Lab, NUST Research Institute for Microwave and Millimeter-Wave Studies (RIMMS) for extending their facility for carrying out EMI shielding measurements of the samples. Similarly, the authors acknowledge the NUST MS Students Research Grant for partial support in purchase of materials and carrying out the characterization of the samples. One of the authors, Dr. Saifullah Awan, acknowledges the financial support from the

https://doi.org/10.1021/acsomega.3c04120
ACS Omega 2024, 9, 3070−3077

Higher Education Commission of Pakistan under Grant No. 5339/Federal/NRPU/R&D/HEC/2015 and the project "Controlled Synthesis of Two-Dimensional Nanosheets and Multilayer for Electronic Devices" for financial support in acquisition of the materials. However, this grant does not cover the costs for the publication charges. The authors also acknowledge the research fund of the National University of Sciences and Technology (NUST) Islamabad, Pakistan for extension of financial support covering the publication charges of this work.

REFERENCES

(1) Sudo, T.; Sasaki, H.; Masuda, N.; Drewniak, J. L. Electromagnetic Interference (EMI) of System-on-Package (SOP). *IEEE Transactions on Advanced Packaging* **2004**, *27*, 304−314.
(2) Geetha, S.; Satheesh Kumar, K. K.; Rao, C. R. K.; Vijayan, M.; Trivedi, D. C. EMI Shielding: Methods and Materials—A Review. *J. Appl. Polym. Sci.* **2009**, *112*, 2073−2086.
(3) Mobius, K.- H. Fullstoffhaltige Elektrisch Leitfahige. *Kunststoffe-German Plastics* **1988**, *78*, 53−58.
(4) Im, J. S.; Kim, J. G.; Lee, S. H.; Lee, Y. S. Effective electromagnetic interference shielding by electrospun carbon fibers involving Fe2O3/BaTiO3/MWCNT additives. *Mater. Chem. Phys.* **2010**, *124*, 434−438.
(5) Jing, X.; Wang, Y.; Zhang, B. Electrical Conductivity and Electromagnetic Interference Shielding of Polyaniline/Polyacrylate Composite Coatings. *J. Appl. Poly. Sci.* **2005**, *98*, 2149−2156.
(6) Al-Saleh, M. H.; Sundararaj, U. Review of the mechanical properties of carbon nanofiber/polymer composites. *Appl. Sci. and Manufact.* **2011**, *42*, 2126−2142.
(7) Nasouri, K.; Salimbeygi, G.; Mazaheri, F.; Malek, R.; Shoushtari, A. M. Fabrication of Polyvinyl Alcohol/Multi-Walled Carbon Nanotubes Composite Electrospun Nanofibers and Their Application as Microwave Absorbing Material. *Micro & Nano Letters* **2013**, *8*, 455−459.
(8) McCullen, S. D.; Stevens, D. R.; Roberts, W. A.; Ojha, S. S.; Clarke, L. I.; Gorga, R. E. Morphological, electrical, and mechanical characterization of electrospun nanofiber mats containing multiwalled carbon nanotubes. *Macromolecule* **2007**, *40*, 997−1003.
(9) Nasouri, K.; Shoushtari, A. M.; Kaflou, A.; Bahrambeygi, H.; Rabbi, A. Single-wall carbon nanotubes dispersion behavior and its effects on the morphological and mechanical properties of the electrospun nanofibers. *Polym. Compos.* **2012**, *33*, 1951−1959.
(10) Feng, X.; Liao, G.; Du, J.; Dong, L.; Jin, K.; Jian, X. Electrical conductivity and microwave absorbing properties of nickel-coated multiwalled carbon nanotubes/poly (phthalazinone other sulfone ketone)s composites. *Polym. Eng. Sci.* **2008**, *48*, 1007−1014.
(11) Rabbi, A.; Nasouri, K.; Bahrambeygi, H.; Shoushtari, A. M.; Babaei, M. R. RSM and ANN approaches for modeling and optimizing of electrospun polyurethane nanofibers morphology. *Fiber Polym.* **2012**, *13*, 1007−1014.
(12) Koombhonges, S.; Liu, W.; Reneker, D. H. Flat polymer ribbons and other shapes by electrospinning. *J. Polym. Sci. Polym. Phys.* **2001**, *39*, 2598−2606.
(13) Makeiff, D. A.; Huber, T. Microwave absorption by polyaniline− carbon nanotube composites. *Synth. Metal* **2006**, *156*, 497−505.
(14) Huang, Z.-M.; Zhang, Y.-Z.; Kotaki, M.; Ramakrishna, S. A Review On Polymer Nanofibers by Electrospinning and their Applications in Nanocomposites. *Compos. Sci. Technol.* **2003**, *63*, 2223−2253.
(15) Frenot, A.; Chronakis, I. S. Polymer Nanofibers Assembled by Electrospinning. *Curr. Opin. Colloid Interface Sci.* **2003**, *8*, 64−75.
(16) Reneker, D. H.; Yarin, A. L.; Zussman, E.; Xu, H. Electrospinning of Nanofibers from Polymer Solutions and Melts. *Adv. Appl. Mech.* **2007**, *41*, 43−346.
(17) Wong, K. K. H.; Zinke-Allmang, M.; Hutter, J. L.; Hrapovic, S.; Luong, J. H. T.; Wan, W. The Effect Of Carbon Nanotube Aspect Ratio And Loading On The Elastic Modulus of Electrospun Poly (Vinyl Alcohol)- Carbon Nanotube Hybrid Fibers. *Carbon* **2009**, *47*, 2571−2578, DOI: 10.1016/j.carbon.2009.05.006.
(18) Wongon, J.; Thumsorn, S.; Srisawat, N. Poly (Vinyl Alcohol)/ Multiwalled Carbon Nanotubes Composite Nanofiber Energy. *Procedia* **2016**, *89*, 313−317.
(19) Kim, M. J.; Lee, J.; Jung, D.; Shim, S. E. Electrospun Poly (Vinyl Alcohol) Nanofibers Incorporating Pegylated Multi-Wall Carbon Nanotube. *Synth. Met.* **2010**, *160*, 1410−1414.
(20) Shoushtari, A. M.; Salimbeygi, G.; Nasouri, K.; Haji, A. Fabrication of Homogeneous Multi-Walled Carbon Nanotube/ Poly (Vinyl Alcohol) Composite Nanofibers for Microwave Absorption. *Application Proc. 3rd Int. Conf. Nano Mater.: Appl. and Prop.*; Sumy State University-Ukraine, 2013; 2, 03NCNN42(1-4).
(21) Strano, M. S.; Moore, V. C.; Miller, M. K.; Allen, M. J.; Haroz, E. H.; Kittrell, C.; Hauge, R. H.; Smalley, R. E. The Role of Surfactant Adsorption During Ultrasonication in the Dispersion of Single-Walled Carbon Nanotubes. *J. Nano Sci. and Nano Technol.* **2003**, *3*, 81−86.
(22) Park, C.; Ounaies, Z.; Watson, K. A.; Crooks, R. E.; Smith, J., Jr.; Lowther, S. E.; Connell, J. W.; Siochi, E. J.; Harrison, J. S.; St Clair, T. L. Dispersion of Single Wall Carbon Nanotubes by in Situ Polymerization Under Sonication. *Chem. Phys. Lett.* **2002**, *364*, 303−308.
(23) Ma, P.-C.; Siddiqui, N. A.; Marom, G.; Kim, J.-K. Dispersion and Functionalization of Carbon Nanotubes for Polymer-Based Nanocomposites: A Review. *Composites Part A: Appl. Sci. and Manufact.* **2010**, *41*, 1345−1367.
(24) Zhao, B.; Du, Y.; Yan, Z.; Rao, L.; Chen, G.; Yuan, M.; Yang, L.; Zhang, J.; Che, R. Structural Defects in Phase-Regulated High-Entropy Oxides towards Superior Microwave Absorption Properties. *Adv. Funct. Mater.* **2023**, *33* (1−13), 2209924.
(25) Zhao, B.; Yan, Z.; Du, Y.; Rao, L.; Chen, G.; Wu, Y.; Yang, L.; Zhang, J.; Wu, L.; Zhang, D. W.; Che, R. High-Entropy Enhanced Microwave Attenuation in Titanate Perovskites. *Adv. Mater.* **2023**, *35* (11), 2210243.
(26) Nasouri, K.; Shoushtari, A. M. Designing modeling and manufacturing of lightweight carbon nanotubes/polymer composite nanofibers for electromagnetic interference shielding application Compos. *Sci. Technol.* **2017**, *145*, 46−54.
(27) Omana, L.; Chandran, A.; John, R. E.; Wilson, R.; George, K. C.; Unnikrishnan, N. V.; Varghese, S. S.; George, G.; Simon, S. M.; Paul, I. Recent Advances in Polymer Nanocomposites for Electromagnetic Interference Shielding: A Review. *ACS Omega* **2022**, *7*, 25921−25947.
(28) Elashmawi, I. S.; Abdel Baieth, H. E. Spectroscopic studies of hydroxyapatite in PVP/PVA polymeric matrix as biomaterial. *Current Appl. Phys.* **2012**, *12*, 141−146.
(29) Lee, Y. M.; Kimt, S. H.; Kimt, S. J. Preparation And Characteristics Of β Chitin And Poly(Vinyl Alcohol). *Blend Polymer* **1996**, *37*, 5897−5905.
(30) Alghunaim, N. S. Optimization and Spectroscopic Studies on Carbon Nanotubes/PVA Nanocomposites. *Results in Phys.* **2016**, *6*, 456−460.
(31) Peng, M.; Qin, F. Clarification of basic concepts for electromagnetic interference shielding effectiveness. *J. Appl. Phys.* **2021**, *130* (1−9), 225108.

https://doi.org/10.1021/acsomega.3c04120
ACS Omega 2024, 9, 3070−3077